*Thermochimica Acta*, 105 (1986) 313–331
Elsevier Science Publishers B.V., Amsterdam – Printed in The Netherlands

# THE EFFECT OF HEAT TRANSPORT WITHIN THE SAMPLE ON THE SHAPE OF THERMOANALYTICAL CURVES

GYÖRGY POKOL, SÁNDOR GÁL and ERNÖ PUNGOR

*Institute for General and Analytical Chemistry, Technical University of Budapest, Budapest, 1521 (Hungary)*

(Received 14 February 1986)

## ABSTRACT

Constant heating rate thermoanalytical curves were simulated for processes governed by a phase boundary reaction and the heat conduction inside the sample. The effects of thermal conductivity, the heat of the reaction, the sample size, etc., on the shape of the peak and on the kinetic parameters estimated without considering thermal resistance are described.

Dimension analysis was applied to obtain quantitative expressions of:

(a) the maximum difference between the temperature of the reacting interface and the program temperature,

(b) the criteria of accurate estimation of kinetic constants without considering heat transport, on the basis of material and experimental parameters.

## INTRODUCTION

Methods of thermal analysis are usually applied in the investigation of solid substances. In kinetic studies based on thermoanalytical curves, the following rate equation is used almost exclusively:

$$\frac{d\alpha}{dt} = A \exp\left(-\frac{E}{RT}\right) f(\alpha) \tag{1}$$

However, eqn. (1) has some formal characteristics; thus the values of the pre-exponential factor and the activation energy are influenced by several material and experimental parameters which are not included in eqn. (1) explicitly. Among others, the specific surface, grain size, structural defects and the pressure belong to these parameters [1]. With a rare exception, the pre-exponential factor $A$, always depends on the sample size [2–4].

It is also well known that the transport processes play an important role in the reactions of solids, and — depending on the parameters of the sample and the experiment — they may be rate-determining for the overall process. Among the f($\alpha$) functions used in eqn. (1), some correspond to diffusion mechanisms [1]. The engineering approach of describing the transformations of large solid samples with defined geometry should be based on the laws of

0040-6031/86/$03.50

heat and component transport and the temperature and concentration gradients in the system [5].

The transport processes were found to determine the character of the decomposition curves of 0.5–50 mg calcium carbonate samples [2].

Resistances to heat transport occur between the heating element and the sample holder, in the wall of the latter, between the sample holder and the sample, and within the sample itself. In the opinion of Paulik and Paulik [6], one of these resistances often determines the rate of the whole process.

The description of the transformation rate worked out by Draper and Sveum [7] corresponds to the case when a chemical reaction takes place in equilibrium conditions at a constant temperature, and the rate of the process is determined by heat transport alone. A similar starting assumption was applied by Meisel et al. [8,9] who studied the operation of DTA cells by means of an electric analog circuit and mathematical simulation.

When the rate of the transformation and the signal of the thermoanalytical instrument are determined by heat transport alone, no information can be obtained on the kinetics of the chemical reaction. Therefore, research workers intend to provide an intensive heat exchange between the sample and the surroundings with the aid of proper instrument design and small samples.

If the heat resistance within the sample is neither dominating nor negligible, the temperature of the reacting substance and its time derivative differ from the temperature measured outside the sample and the chosen heating rate, respectively. The actual temperature, which is not uniform in the sample, is unknown. Usually, the measured curve is evaluated using eqn. (1) with the assumption that the temperature of the sample obeys the linear program. In this case, according to Šesták [10], deviation from the temperature program can be regarded as an error source of the estimated kinetic parameters. In the same work, Šesták also suggested approximate equations for the temperature difference between the surface and the center of disk-shaped or cylindrical samples. The error caused by the deviation from the ideal temperature program was studied by Várhegyi in detail. First he pointed out that neglecting the temperature difference in question distorts the shape of the curve and a 5 K temperature difference within the sample results in unacceptable errors of the estimated kinetic constants [11]. Substituting

$$f(\alpha) = (1 - \alpha)^n \qquad (2)$$

in eqn. (1), he described the sign of the error of the estimated apparent order depending on the convex or concave character of the real $T(t)$ function [12], and specified error bounds of the activation energy and the formal order [13]. Reich and Stivala investigated the degradation of Teflon [14]. Their cylindrical samples were embedded in a thermal insulator so that only one of the faces was exposed. They found that, for lower conversions, the decomposition could be described by a mathematical model taking into account the rate of the chemical reaction and one-dimensional heat conduction.

In the present work, we intend to answer the following questions:

(a) How do the parameters related to heat transport (sample size, heat of reaction, thermal conductivity, heating rate, etc.) influence the shape of thermoanalytical curves?

(b) What is the effect of neglecting the thermal resistance of the sample on the estimated kinetic parameters?

(c) What conditions should be satisfied by the parameters of the reaction and the experiment for acceptable reliability if the kinetic constants are estimated without considering thermal resistance?

These problems were studied by means of simulated, constant heating rate curves. In the following, the part of the thermoanalytical curve belonging to the reaction will be called a peak, though the model and the results concern both differential and integral curves.

The mathematical model corresponds to a process whose rate is determined by a three-dimensional phase boundary (contracting envelope) reaction and the heat conduction within the sample.

The shape of the simulated peaks was characterized by empirical parameters discussed in detail in previous works [15–18]. The definitions of the empirical parameters used here are listed in the Notation section. Each of these quantities can be related to a property of the peak as the position along the temperature axis ($T(\mathrm{Max})$; $M_{1\mathrm{R}}$), width ($\Delta T(0.8, 0.2)$, $W$), sharpness ($U$) or asymmetry ($\alpha(\mathrm{Max})$, $R(0.6)$). The empirical parameters mentioned were appied in the investigation of the reproducibility of experimental DSC curves [15], of the effect of noises and baseline [16] and that of the possibility to estimate kinetic parameters [17,18].

## CALCULATIONS

### *The mathematical model*

Let us consider a reaction of a solid substance whose products include at least one solid, e.g. $\mathrm{solid}_1 = \mathrm{solid}_2 + \mathrm{gas}$. If the solid phases are pure, there is a reacting phase boundary moving toward the interior of the sample (contracting envelope). The heat required for the transformation reaches the reacting phase boundary through the porous solid product. (A number of real processes belong to this class, e.g. the decomposition of metal carbonates and hydroxides.)

The basic assumptions of the model are:

(1) The overall rate of the process is determined by the chemical reaction at the moving boundary and the heat conduction within the sample (i.e. both the thermal resistances outside the sample and the resistance to mass transport are negligible).

(2) The heat flux into (or out of) the sample is equal to the heat effect of the reaction.

Assumption (2) is equivalent to neglecting the heat capacity of the sample; in other words, the heat required for the change of sample temperature is not taken into account. A coarse estimate of the fraction neglected in this way can be obtained as follows.

Let the temperature range where the transformation rate is significant be 50 K, the heat of reaction 40–100 kJ $\text{mol}^{-1}$ and the molar heat capacity 50–200 J $\text{mol}^{-1}$ $\text{K}^{-1}$ (being real in the field of inorganic substances). Starting from these values, the enthalpy change of heating amounts to 2.5% of the heat effect of the reaction in the most favorable case and to 25% in the worst. Thus, neglecting the heat capacity seems an acceptable approximation for a number of reactions.

Besides, the model includes some further simplifications and limiting conditions. The chemical reaction is assumed to proceed far from equilibrium (excluding the reverse reaction); the density, heat of reaction and thermal conductivity are treated as constants during the transformation. A spherical sample geometry was chosen. Real experimental conditions are often close to this; in such cases $n = 2/3$ is valid in eqn. (2).

At a specific moment, when the radius and temperature of the reacting (spherical) phase boundary are known, the rate of transformation can be expressed in the form

$$\frac{\mathrm{d}N}{\mathrm{d}t} = 4r^2\pi A' \exp\left(-\frac{E}{RT}\right) \tag{3}$$

If we apply eqns. (1) and (2) to our case, as usual in the field of thermal analysis,

$$\frac{\mathrm{d}\alpha}{\mathrm{d}t} = A \exp\left(-\frac{E}{RT}\right)(1-\alpha)^{2/3} \tag{4}$$

is obtained. The pre-exponential coefficients of eqns. (3) and (4) are not identical, as pointed out in our previous works [2–4], their dimensions are also different (see the Notation section). In order to obtain the velocity ($v$) of the advancing reacting phase boundary, let us express the rate of transformation as (kg $\text{s}^{-1}$):

$$\frac{\mathrm{d}N}{\mathrm{d}t}M = -4r^2\pi\frac{\mathrm{d}r}{\mathrm{d}t}\rho \tag{5}$$

After rearrangement, this yields

$$v = -\frac{\mathrm{d}r}{\mathrm{d}t} = -\frac{A'M}{\rho}\exp\left(-\frac{E}{RT}\right) \tag{6}$$

The heat flux reaching the reacting boundary can be calculated from the rate of transformation and from the temperature difference between the outer surface of the sample and the reacting boundary. Let us distinguish these values by indices v and $\lambda$, respectively, though $\dot{Q}_v$ and $\dot{Q}_\lambda$ must be equal, according to basic assumption (2).

$$\dot{Q}_v = 4r^2\pi A' \exp\left(-\frac{E}{RT}\right) \Delta H \tag{7}$$

$$\dot{Q}_\lambda = 4\pi\lambda r_0 r \frac{T(r_0) - T}{r_0 - r} \tag{8}$$

Equation (8) corresponds to the heat conduction through the spherical shell between the outer surface and the reacting phase boundary, if the outer radius is unchanged during the reaction. Taking into account basic assumption (1), $T(r_0)$ is always equal to the program temperature.

### *The simulation procedure*

The basic equations discussed in the preceding section are sufficient to calculate the temperature of the outer surface, the radius, temperature and velocity of the reacting phase boundary at time $t$ ($T(r_0)$, $T$, $r$ and $v$, respectively), if their values are known a little earlier, at $t - \Delta t$ ($T'(r_0)$, $T'$, $r'$ and $v'$). Figure 1 shows the block diagram of the iteration procedure worked out for this purpose.

The temperature of the outer surface is

$$T(r_0) = T'(r_0) + \beta \, \Delta t \tag{9}$$

The starting values of the temperature and radius of the reacting interface are

$$r_1 = r' - v' \, \Delta t \tag{10}$$

$$T_1 = T' \tag{11}$$

Substituting $r_1$ and $T_1$ into eqn. (7), $\dot{Q}_v$ is obtained. Then, using this value as $\dot{Q}_\lambda$, a new temperature ($T_2$) is calculated from eqn. (8). Now, if we are close enough to the values adequate to basic assumption (2), the absolute difference of the first and second temperatures will be lower than a preselected limit

$$\delta T_1 = | T_2 - T_1 | < \epsilon \tag{12}$$

Otherwise, if eqn. (12) does not hold, $T_2$ is chosen as the temperature of the reacting phase boundary, and the iteration is repeated from calculated $\dot{Q}_v$ (see version a in Fig. 1). These steps can be repeated until the actual $\delta T_i$ value becomes lower than $\epsilon$.

Depending on the parameters, the iteration steps outlined here may lead to increasing $\delta T_i$ values. In this case, a reverse order of steps should be followed: first $\dot{Q}_\lambda$ is calculated from $T_i$ accordingly to eqn. (8), then this heat flux is substituted for $\dot{Q}_v$ in eqn. (7) and a new temperature is obtained (version b, Fig. 1).

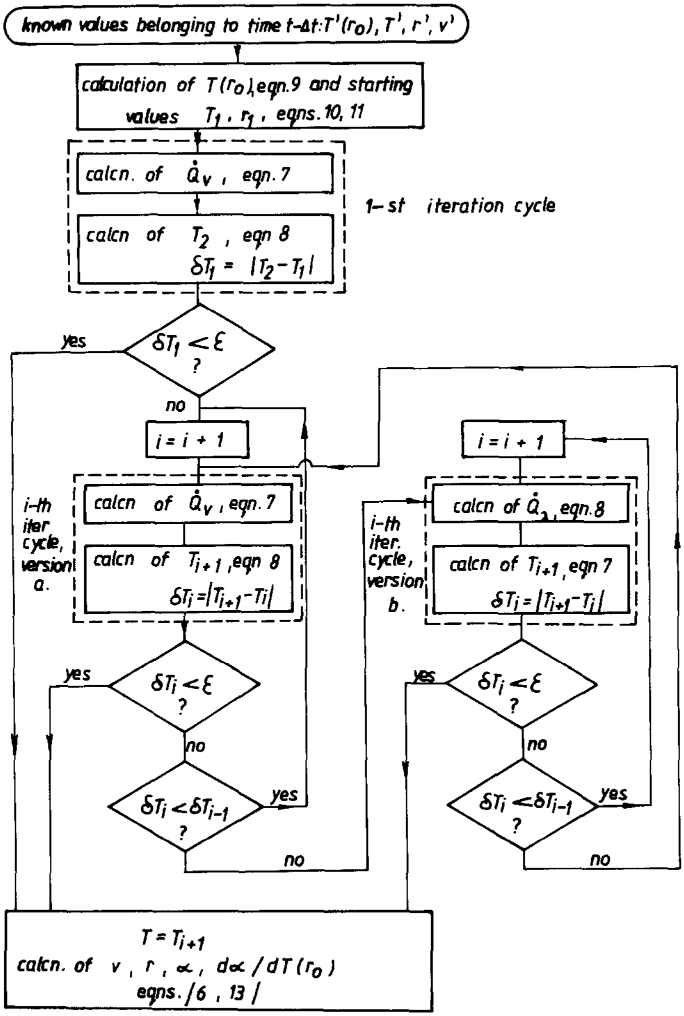

Fig. 1. Block diagram of the iteration procedure.

At the end of the iteration when we have an acceptable value of $T_{i+1}$, this value is regarded as the correct temperature of the reacting phase boundary ($T$), and the velocity determined by eqn. (6) is used to calculate the radius of the reacting boundary at time $t$:

$$r = r' - v\,\Delta t \tag{13}$$

Now $\alpha$ and $d\alpha/dt$ needed in the evaluation of peak shape can also be obtained.

The procedure outlined here may be applied in a step-by-step manner to generate the whole peak, starting from a suitably low temperature. Two remarks should be made to this point.

(a) Mathematically possible sets of parameters render the iteration of the reacting phase boundary divergent. However, during the simulations, within the ranges of parameters applied in the present work, an acceptable accuracy could always be achieved (e.g. $\delta T_i < 0.01$ K when the temperature difference between the outer surface and the reacting phase boundary amounted to several Kelvin).

(b) Some errors may be accumulated in recoursive procedures. In order to check this effect, curves generated by this procedure, using a very high thermal conductivity, were compared to curves generated by a proven program based on eqn. (4). If the distance of adjacent points satisfied the $\beta\ \Delta t \leqslant 1$ K condition, the two curves agreed reasonably well.

### *Evaluation*

In the characterization of the simulated peaks, the empirical parameters discussed in earlier works [15–18] and mentioned in the Introduction were applied. In the calculation the points of the simulated curves were given by the program temperature ($T(r_0)$), the reacted fraction ($\alpha$) and the $\mathrm{d}\alpha/\mathrm{d}T(r_0)$ rate; the latter equals $\beta^{-1}(\mathrm{d}\alpha/\mathrm{d}t)$. Besides, the difference between the temperature of the external surface and that of the reacting phase boundary was also followed.

The calculations were carried out on an HP-85A personal computer; the same program contained the simulation and the evaluation of curves.

### *The ranges of input parameters*

The parameters of the reaction and the "experiment" were chosen to represent real cases occurring in the field of thermal analysis. Thermal conductivity, sample radius and heating rate were varied in wide ranges. Besides, two pre-exponential factor–activation energy pairs were used, resulting in peaks of considerably different width. Changing the reaction heat was not needed as — taking into account the form and the use of eqns. (7) and (8) — the $\lambda/\Delta H$ ratio is of interest.

The real range of the thermal conductivity is below 10 W m$^{-1}$ K$^{-1}$. At several hundred Kelvin, metals and alloys only possess higher $\lambda$ values [19]. Moreover, in the present model, heat transport takes place through a porous layer, even if the sample is originally compact. Thus, an effective thermal conductivity lower than the $\lambda$ value of the compact substance should be considered. Among porous refractory materials, thermal conductivities in the order of 0.1 W m$^{-1}$ K$^{-1}$ are not exceptional [19].

## RESULTS AND DISCUSSION

### *The effect of sample size, thermal conductivity and heating rate on peak shape*

Several empirical parameters characteristic of peak shape are summarized in Table 1 for curves simulated with different thermal conductivities. The

TABLE 1

The effect of thermal conductivity on the parameters of peak shape, in the case of $A' = 4.72 \times 10^{12}$ mol m$^{-2}$ s$^{-1}$; $E/R = 1.670 \times 10^4$ K, $\beta = 1/6$ K s$^{-1}$, $M = 0.1$ kg mol$^{-1}$, $\rho = 2000$ kg m$^{-3}$, $\Delta H = 100$ kJ mol$^{-1}$ and $r_0 = 3$ mm

| $\lambda$ (W K$^{-1}$ m$^{-1}$) = | $\infty$ | 100 | 20 | 5 | 1 | 0.2 |
|---|---|---|---|---|---|---|
| $T$(Max)(K) | 541.5 | 541.5 | 541.5 | 540.5 | 540.5 | 541.8 |
| $M_{1R}$ (K) | 530.6 | 530.7 | 530.8 | 531.4 | 533.8 | 542.1 |
| $T$(0.2) (K) | 517.6 | 517.6 | 517.6 | 517.6 | 517.9 | 519.1 |
| $T$(0.8) (K) | 545.6 | 545.7 | 546.0 | 547.0 | 551.5 | 556.7 |
| $W$ (K) | 38.3 | 38.4 | 39.1 | 41.3 | 49.8 | 73.1 |
| $\Delta T$(0.8, 0.2) (K) | 28.0 | 28.1 | 28.4 | 29.3 | 33.5 | 47.6 |
| $\alpha$(Max) | 0.692 | 0.691 | 0.686 | 0.645 | 0.587 | 0.489 |
| $R$(0.6) | 0.731 | 0.730 | 0.727 | 0.719 | 0.691 | 0.647 |
| $l$ | – | 0.3 | 1.3 | 4.4 | 17.5 | 51.6 |

other material and experimental constants are fixed. Figure 2 demonstrates the corresponding rate curves and the curves of the difference between the temperature of the outer sample surface and that of the reacting interface. The maximum values ($l$) of this difference are shown in the last row of Table 1. Note that $T(r_0)$, i.e. program temperature, appears on the abcissa and in the expression of the transformation rate in Fig. 2. Thus, the rate curves are equivalent to $d\alpha/dt$ vs. $t$ curves.

Using the data in Table 1 the effect of decreasing thermal conductivity can be characterized as follows. The higher the fraction reacted, the greater is the shift of $T(\alpha)$ values compared to those belonging to $\lambda = \infty$. The effect of $\lambda$ on the peak maximum temperature and the first relative moment is relatively small. The empirical parameters related to peak width ($W$ and $\Delta T(0.8, 0.2)$) show a considerable increase as $\lambda$ decreases. Similarly, quantities related to peak asymmetry ($\alpha$(Max) and $R(0.6)$) are quite sensitive to the thermal conductivity. The data demonstrated in Table 1 belong to a sample radius of 3 mm; i.e., using the density given in the heading, to an initial sample mass of 230 mg. Similar series of curves were generated with sample radii of 10, 1 and 0.3 mm, corresponding to 8.4 g, 8.4 mg and 0.23 mg initial mass, respectively. The first relative moment, the reciprocal of the maximum transformation rate, and the $R(0.6)$ ratio of these peaks are included in Table 2.

The maximum difference between the temperature of the external surface and the reacting interface is shown in Figs. 3 and 4 as a function of the thermal conductivity and the sample radius, respectively.

In order to assess $l$, it may be compared to the width of the peak. In the case of $r_0 = 3$ mm and $\lambda = 5$ W K$^{-1}$ m$^{-1}$ the maximum difference exceeds 10% of the $W$ value belonging to $\lambda = \infty$ (see Table 1). For $r_0 = 0.3$ mm, $l$ reaches this ratio at about 0.05 W K$^{-1}$ m$^{-1}$ (Table 2).

In a previous study [17,18] three empirical parameters, related to the position, the width and the sharpness or the asymmetry of the peak (e.g. $M_{1R}$, $W$ and $R(0.6)$) were found suitable for the estimation of $A$, $E$ and $n$ if eqns. (1) and (2) were valid.

Let us consider the data in Table 1. In the case of a fixed sample radius, $\lambda$ and $R(0.6)$ change in the same sense. As shown in the works mentioned before [17,18], lower values of $R(0.6)$ belong to higher formal order, and this relationship can be applied in the estimation of $n$. For example, $R(0.6) = 0.703$ yields $n = 1$.

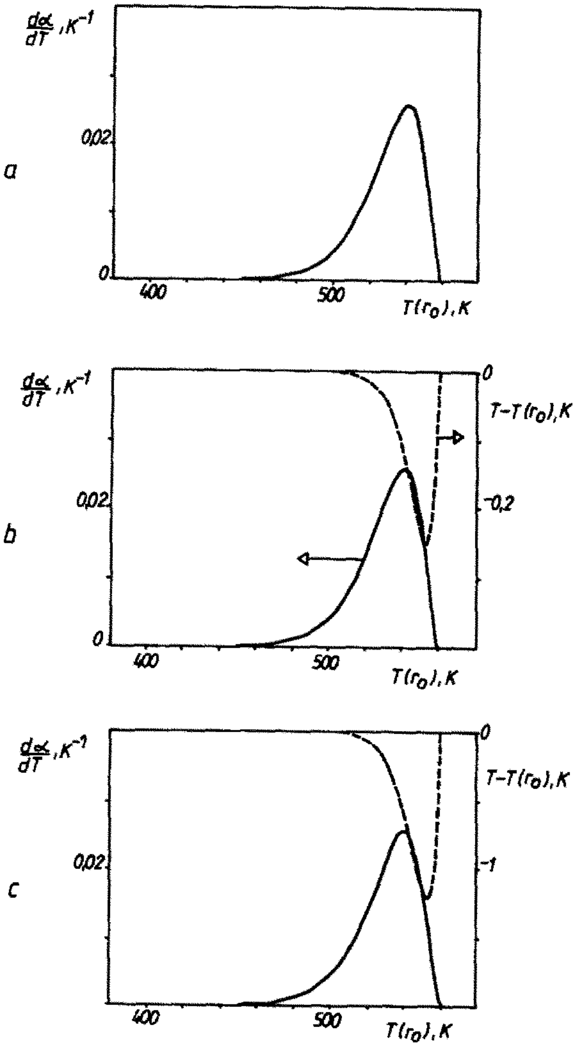

Fig. 2. Curves of the transformation rate (———) and the difference between the temperature of the reacting phase boundary and the program temperature (— — —) for a sample of 3 mm initial radius. For the other parameters of simulation see the heading of Table 1. $\lambda$ (W K$^{-1}$ m$^{-1}$) = (a) $\infty$, (b) 100, (c) 20, (d) 5, (e) 1, (f) 0.2.

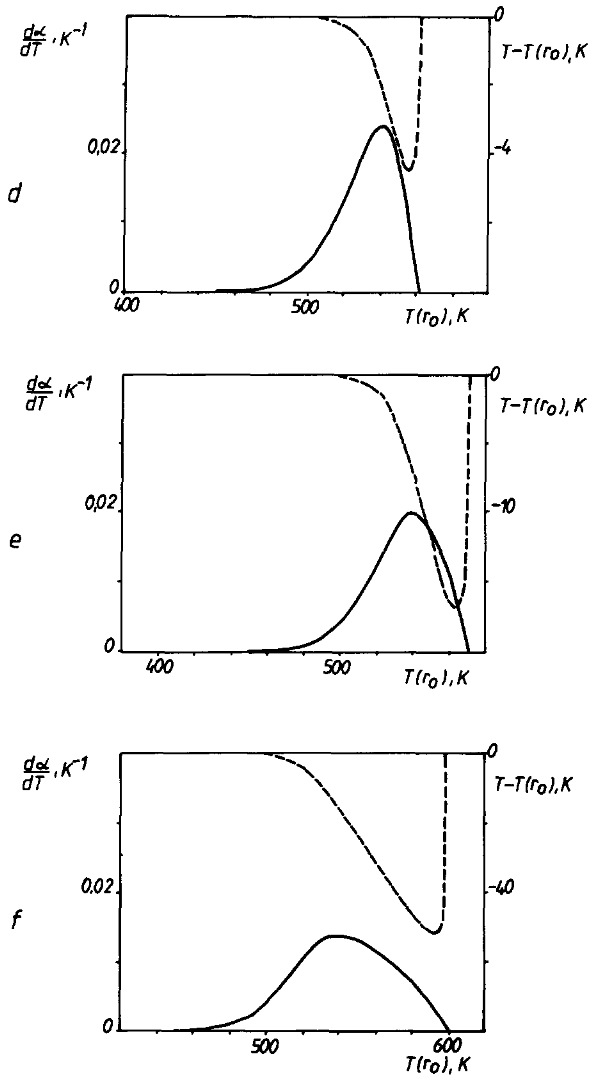

Fig. 2 (continued).

From Fig. 5, showing the effect of the thermal conductivity on this ratio, the $\lambda$ value resulting in $R(0.6) = 0.703$ can be determined; it is 2.2 W K$^{-1}$ m$^{-1}$. This means that if our model process takes place in a sample of $r_0 = 3$ mm and $\lambda = 2.2$ W K$^{-1}$ m$^{-1}$, and the thermal resistance is neglected in the evaluation of the transformation rate, a formal order of 1 will be obtained instead of 2/3, the correct value. Besides, the error of $n$ also influences the estimated activation energy and pre-exponential factor.

In a similar way, a minimum effective thermal conductivity can be determined for a particular set of material constants, sample radius and experimental circumstances. If the acceptable error of the estimated $n$ value

TABLE 2

Some of the parameters characterizing peak shape and maximum temperature lag for samples of different initial radius and thermal conductivity (for other starting parameters see heading of Table 1)

| $r_0$ (mm) | $\lambda$ ($\mathrm{W\,K^{-1}\,m^{-1}}$) | $M_{1R}$ (K) | $W$ (K) | $R(0.6)$ | $l$ (K) |
|---|---|---|---|---|---|
| 10 | ∞ | 550.5 | 41.1 | 0.730 | – |
| | 100 | 550.9 | 42.7 | 0.724 | 2.5 |
| | 20 | 552.3 | 47.9 | 0.707 | 10.2 |
| | 5 | 556.3 | 60.9 | 0.674 | 29.8 |
| | 1 | 570.5 | 102.2 | 0.632 | 66.5 |
| 3 | ∞ | 530.5 | 38.3 | 0.731 | – |
| | 100 | 530.7 | 38.4 | 0.730 | 0.3 |
| | 20 | 530.8 | 39.1 | 0.727 | 1.3 |
| | 5 | 531.4 | 41.3 | 0.719 | 4.4 |
| | 1 | 533.8 | 49.8 | 0.691 | 17.5 |
| | 0.2 | 542.1 | 73.1 | 0.647 | 51.6 |
| 1 | ∞ | 513.7 | 36.0 | 0.731 | – |
| | 5 | 513.8 | 36.3 | 0.729 | 0.6 |
| | 1 | 514.1 | 37.8 | 0.723 | 2.8 |
| | 0.2 | 515.7 | 43.5 | 0.702 | 11.2 |
| | 0.05 | 520.0 | 56.4 | 0.668 | 30.8 |
| 0.3 | ∞ | 496.3 | 33.6 | 0.731 | – |
| | 1 | 496.3 | 33.8 | 0.730 | 0.3 |
| | 0.2 | 496.5 | 34.5 | 0.727 | 1.4 |
| | 0.05 | 497.1 | 37.0 | 0.717 | 5.0 |

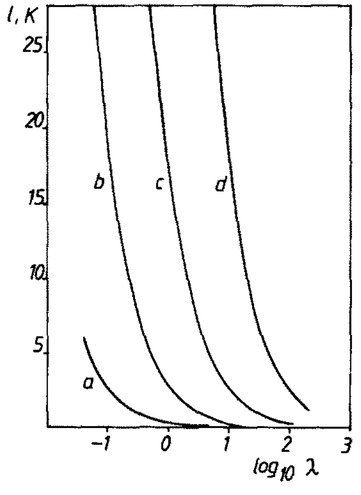

Fig. 3. The effect of the thermal conductivity on the maximum temperature difference between the outer surface and the reacting phase boundary. For the parameters of simulation see the heading of Table 1. $r_0$ (mm) = (a) 0.3, (b) 1, (c) 3, (d) 10.

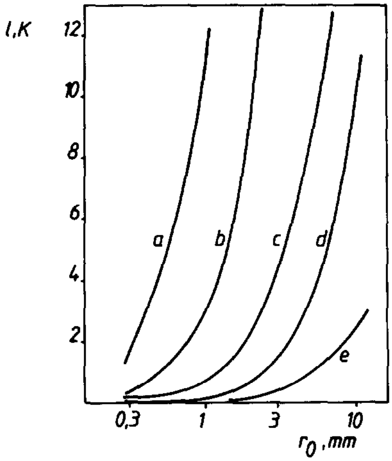

Fig. 4. The effect of the sample radius on the maximum temperature lag. For the parameters of simulation see the heating of Table 1. λ (W $K^{-1}$ $m^{-1}$) = (a) 0.2, (b) 1, (c) 5, (d) 20, (e) 100.

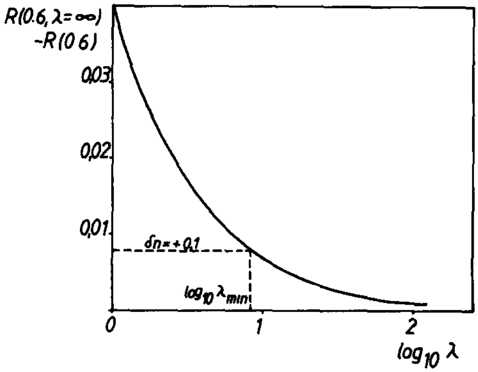

Fig. 5. The effect of the thermal conductivity on the shift of $R(0.6)$ for a sample of 3 mm radius. For the other parameters of simulation see the heading of Table 1.

TABLE 3

The effect of thermal conductivity on the parameters of peak shape, in the case of a narrower peak: $A' = 2 \times 10^{25}$ mol $m^{-2}$ $s^{-1}$; $E/R = 3.293 \times 10^4$ K, $r_0 = 3$ mm (for other starting parameters, see the heading of Table 1)

| λ (W $K^{-1}$ $m^{-1}$) | $M_{1R}$ (K) | $W$ (K) | $R(0.6)$ | $l$ (K) |
|---|---|---|---|---|
| ∞ | 548.9 | 21.4 | 0.735 | – |
| 100 | 548.9 | 21.7 | 0.733 | 0.4 |
| 20 | 549.2 | 22.8 | 0.725 | 2.1 |
| 5 | 550.1 | 26.1 | 0.704 | 6.8 |
| 1 | 553.6 | 36.4 | 0.662 | 21.7 |

TABLE 4

The effect of heating rate on some parameters characterizing peak shape and the maximum temperature lag, in the case of $r_0 = 1$ mm sample radius (for other starting parameters of simulation, see the heading of Table 1)

| $\beta$ ($K\,s^{-1}$) | $\lambda$ ($W\,K^{-1}\,m^{-1}$) | $M_{1R}$ (K) | $W$ (K) | $R(0.6)$ | $l$ (K) |
|---|---|---|---|---|---|
| 1/12 | ∞ | 503.5 | 34.6 | 0.731 | – |
| | 5 | 503.6 | 34.8 | 0.730 | 0.3 |
| | 1 | 503.7 | 35.6 | 0.727 | 1.5 |
| | 0.2 | 504.6 | 38.9 | 0.713 | 6.5 |
| 1/3 | ∞ | 524.2 | 37.4 | 0.731 | – |
| | 5 | 524.4 | 38.1 | 0.728 | 1.1 |
| | 1 | 525.1 | 40.7 | 0.718 | 5.0 |
| | 0.2 | 527.8 | 50.0 | 0.688 | 18.9 |
| 1 | ∞ | 541.9 | 39.8 | 0.730 | – |
| | 20 | 542.0 | 40.4 | 0.728 | 0.8 |
| | 5 | 542.4 | 41.8 | 0.723 | 3.0 |
| | 1 | 544.0 | 48.0 | 0.702 | 12.2 |

is 0.1, the $R(0.6)$ ratio should not be lower than 0.723, being 0.008 lower than the value belonging to $n = 2/3$. Starting from this difference, $\lambda_{\min} = 7.9$ $W\,K^{-1}\,m^{-1}$ is obtained from the curve of Fig. 5. If the thermal conductivity

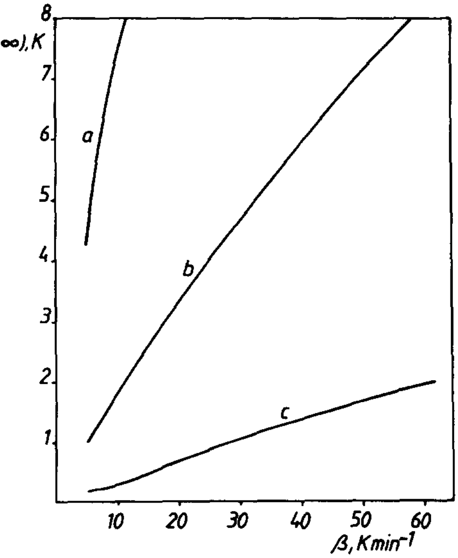

Fig. 6. The effect of the heating rate on the shift of $W$ (related to peak width), in the case of $r_0 = 1$ mm sample radius. For the other starting parameters, see the heading of Table 1. $\lambda$ ($W\,K^{-1}\,m^{-1}$) = (a) 0.2, (b) 1, (c) 5.

exceeds this value, neglecting the thermal resistance (i.e. an estimation based on eqns. (1) and (2)) will result in an error of the estimated $n$ lower than 0.1 for the given set of material and experimental parameters.

The shape of the peak is also affected by the activation energy and the pre-exponential factor, determining the width of the temperature range of the transformation. The values in Table 3, belonging to narrower curves, can be compared to those in Table 1. As is expected, the distorting effect of heat transport becomes stronger with decreasing width of the peak.

The dependence of peak shape on the heating rate was also studied. Results obtained with $r_0 = 1$ mm and different rates are included in Table 4. An empirical parameter related to peak width is illustrated in Fig. 6 as a function of the heating rate.

### *The application of dimension analysis to characterize the effect of heat transport inside the sample*

The results described in the preceding section show the effect of individual material and experimental parameters on the peak shape, provided the other parameters are fixed. Let us consider if these relationships can be formulated generally. In other words, we are seeking answers to the following.

(a) Is it possible to estimate the maximum difference between the temperature of the outer surface and that of the reacting phase boundary if the material and experimental parameters are known?

(b) It is possible to specify the approximate range of material and experimental parameters allowing the kinetic constants of the reaction to be estimated without considering the heat transport (with a given error bound)?

Dimension analysis was applied to solve these problems.

First, let us consider the maximum temperature lag $l$ as a function of the sample size, the thermal conductivity, the heating rate, the heat effect and the width of the temperature range of the reaction. The last two factors may be described by the heat of reaction in unit sample volume,

$$H = \frac{\Delta H}{M} \rho \tag{14}$$

and the reciprocal of the maximum transformation rate $W$. Besides, let us assume that the relationship can be expressed as

$$l = \text{const}\ r_0^a W^b H^c \lambda^d \beta^e \tag{15}$$

The dimensions of the parameters of the right-hand side are $[L]$, $[T]$, $[EL^{-3}]$, $[EL^{-1}T^{-1}\theta^{-1}]$ and $[T\theta^{-1}]$, respectively. The four basic dimensions offer four equations for the exponents $a$–$e$:

$$[T]: \quad 1 = b + e - d \tag{16}$$

$$[L]: \quad 0 = a - 3c - d \tag{17}$$

$$[\theta]: \quad 0 = d + e \tag{18}$$

$$[E]: \quad 0 = c + d \tag{19}$$

Consequently, there is one independent exponent. Let us choose $c$, then the others can be expressed with it. We get $a = 2c$, $b = 1 - 2c$, $d = -c$ and $e = c$. Taking the character of the model process into account, the maximum temperature lag is expected to be (nearly) proportional to the heat of reaction, which corresponds to $c = 1$. Using this value, eqn. (15) becomes

$$l = \text{const}\,\frac{r_0^2 H\beta}{W\lambda} \tag{20}$$

Equation (20) can be verified by calculating $lW\lambda/(r_0^2 H\beta)$ from the data of different simulated curves, when both the chemical reaction and the heat transport play a significant role in the overall rate of the transformation. The results of these calculations (see Table 5) show that eqn. (20) is approximately valid, its constant being about 0.30.

The range of parameters allowing the kinetic constants to be estimated without considering the heat transport can be approached in a similar way. In the preceding section ("The effect of sample size ...") a minimum thermal conductivity has been defined allowing the estimation of the formal order with $\delta n = 0.1$ maximum error. Now let us express $\lambda_{\min}$ with sample radius, width of the reaction temperature range, heat effect and heating rate

$$\lambda_{\min} = \text{const}'\, r_0^{a'} W^{b'} H^{c'} \beta^{d'} \tag{21}$$

Of course, any other parameter of eqn. (21) could be chosen as the explicit variable, i.e. instead of $\lambda_{\min}$, $r_{0,\mathrm{Max}}$ or $W_{\min}$, etc., could be expressed.

As the number of unknown exponents is equal to that of the basic dimensions, equations similar to (16)–(19) can be solved, and $a' = 2$, $b' = -2$, $c' = d' = 1$ is obtained. Substituting these values into eqn. (21) and rearranging yields

$$\frac{\lambda_{\min} W^2}{r_0^2 H\beta} = \text{const}' \tag{22}$$

The constant on the right-hand side of eqn. (22) should be determined from each series of curves simulated with different thermal conductivity and other parameters fixed. $\lambda_{\min}$ can be determined from $R(0.6)$ vs. log $\lambda$ diagrams as shown in Fig. 5, similarly, $W$ is obtained from $W$ vs. log $\lambda$ diagrams created from the data of Tables 2–4. The results of these calculations are included in Table 6; the values of the constant in question are in the range 3.8–4.3, confirming the approximate validity of eqn. (22). Of

TABLE 5

Values of the constant of eqn. (20) calculated from different series of simulated curves

(a) Peaks generated with different radius and thermal conductivity:
$A' = 4.72 \times 10^{12}$ mol m$^{-2}$ s$^{-1}$; $E/R = 1.67 \times 10^4$ K; $\beta = 1/6$ K s$^{-1}$

| $\lambda$ (W K$^{-1}$ m$^{-1}$) | $\frac{lW\lambda}{Hr_0^2\beta}$ | | | |
|---|---|---|---|---|
| | $10^3 r_0$ (m) = 10 | 3 | 1 | 0.3 |
| 100 | 0.32 | 0.32 | | |
| 20 | 0.29 | 0.33 | 0.22 | |
| 5 | 027 | 0.30 | 0.33 | 0.56 |
| 1 | | 0.29 | 0.32 | 0.34 |
| 0.2 | | | 0.29 | 0.32 |
| 0.05 | | | 0.26 | 0.31 |

(b) Peaks generated with different heating rate:
$A' = 4.72 \times 10^{12}$ mol m$^{-2}$ s$^{-1}$; $E/R = 1.67 \times 10^4$ K; $r_0 = 10^{-3}$ m

| $\lambda$ (W K$^{-1}$ m$^{-1}$) | $\frac{lW\lambda}{Hr_0^2\beta}$ | | | |
|---|---|---|---|---|
| | $\beta$(K s$^{-1}$) = 1/12 | 1/6 | 1/3 | 1 |
| 20 | | | | 0.32 |
| 5 | 0.31 | 0.33 | 0.31 | 0.31 |
| 1 | 0.32 | 0.32 | 0.31 | 0.29 |
| 0.2 | 0.30 | 0.29 | 0.28 | |

(c) Narrower peaks generated with different thermal conductivity:
$A' = 2 \times 10^{25}$ mol m$^{-2}$ s$^{-1}$; $E/R = 3.293 \times 10^4$ K; $\beta = 1/6$ K s$^{-1}$; $r_0 = 3 \times 10^{-3}$ m

| $\lambda$(W K$^{-1}$ m$^{-1}$) | 100 | 20 | 5 | 1 |
|---|---|---|---|---|
| $\frac{lW\lambda}{Hr_0^2\beta}$ | 0.29 | 0.32 | 0.30 | 0.27 |

course, instead of a maximum acceptable thermal conductivity, a maximum sample size or heat of reaction may also be interesting. So, in general, we can write

$$\left(\frac{\lambda W^2}{r_0^2 H\beta}\right)_{\min} = \text{const}' \tag{23}$$

where the actual value depends on the selected error limit.

As an example, let us estimate the maximum allowable sample size belonging to 0.1 error of formal order when we can use 4.0 as the value of const′ of eqn. (23). Let the parameters be $\Delta H = 100$ kJ mol$^{-1}$, $\rho = 2000$ kg m$^{-3}$, $M = 0.1$ kg mol$^{-1}$, $\lambda = 1$ W K$^{-1}$ m$^{-1}$, $W = 40$ K and $\beta = 1/6$ K s$^{-1}$. Then, from eqns. (14) and (23), $r_0 = 1.1$ mm is obtained corresponding to a maximum sample mass of 11 mg.

TABLE 6

The values of the constant of eqn. (22) and the maximum allowable $l/W$ ratio calculated from different series of simulated curves

(a) Peaks generated with different radius and thermal conductivity:
$A' = 4.72\times10^{12}$ mol m$^{-2}$ s$^{-1}$; $E/R = 1.67\times10^{4}$ K; $\beta = 1/6$ K s$^{-1}$

| $10^3 r_0$ (m) | 10 | 3 | 1 | 0.3 |
|---|---|---|---|---|
| $\lambda_{\min}$ (W K$^{-1}$ m$^{-1}$) | 76 | 7.9 | 1.0 | 0.089 |
| $\dfrac{\lambda_{\min} W^2}{H r_0^2 \beta}$ | 4.2 | 4.3 | 4.3 | 3.8 |
| $(\frac{l}{W})_{\text{Max}}$ (%) | 7.2 | 8.2 | 7.4 | 8.7 |

(b) Peaks generated with different heating rate:
$A' = 4.72\times10^{12}$ mol m$^{-2}$ s$^{-1}$; $E/R = 1.67\times10^{4}$ K; $r_0 = 10^{-3}$ m

| $\beta$ (K s$^{-1}$) | 1/12 | 1/6 | 1/3 | 1 |
|---|---|---|---|---|
| $\lambda_{\min}$ (W K$^{-1}$ m$^{-1}$) | 0.50 | 1.0 | 1.8 | 4.5 |
| $\dfrac{\lambda_{\min} W^2}{H r_0^2 \beta}$ | 4.0 | 4.3 | 4.2 | 4.0 |
| $(\frac{l}{W})_{\text{Max}}$ (%) | 7.7 | 7.4 | 7.6 | 7.8 |

(c) Narrower peaks generated with different thermal conductivity:
$A' = 2\times10^{25}$ mol m$^{-2}$ s$^{-1}$; $E/R = 3.293\times10^{4}$ K; $\beta = 1/6$ K s$^{-1}$; $r_0 = 3\times10^{-3}$ m

$\lambda_{\min} = 23$ W K$^{-1}$ m$^{-1}$; $\dfrac{\lambda_{\min} W^2}{H r_0^2 \beta} = 3.9$; $(\frac{l}{W})_{\text{Max}} = 8.4\%$

Combining eqns. (20) and (23), the criterion of accurate estimation of kinetic parameters can also be expressed as the ratio of the maximum temperature lag and the width of the reaction temperature range $l/W$. The values of this ratio also show good agreement for the different sets of simulated curves (see Table 6). Thus, for a given accuracy of the estimation based on eqns. (1), (2) or (3), the maximum difference between the temperature of the reacting interface and the program temperature should not exceed a certain percentage of the width of the reaction temperature range (in our example, 7–8%).

Finally, some remarks can be made on the possibility of generalizing the conclusions of the present discussion. Taking into account the simplifications of the model and the special geometric conditions, the conclusions above may only be approximately valid for real transformations governed by the rate of a phase boundary reaction and the heat transport inside the sample. Certainly, the criteria of accurate estimations without considering heat transport are somewhat stricter than those obtained in the present calculations because of the other factors neglected here. However, their order of magnitude can be expected to be correct for a number of processes taking place under the usual circumstances of thermal analysis.

## ACKNOWLEDGMENTS

The authors express their thanks to Dr. G. Vårhegyi and Dr. G.E. Veress for helpful discussions.

## NOTATION

| | |
|---|---|
| $t$ | time |
| $r$ | radius of the reacting phase boundary at time $t$ |
| $r_0$ | sample radius |
| $v$ | the velocity of the reacting phase boundary at time $t$ |
| $T$ | temperature of reacting phase boundary at time $t$ |
| $T(r_0)$ | temperature at the external surface of the sample at time $t$ |
| $\alpha$ | reacted fraction |
| $f(\alpha)$ | a function of $\alpha$ in the rate equation |
| $A$ | pre-exponential factor ($s^{-1}$) see eqns. (1) and (4) |
| $A'$ | pre-exponential factor (mol $m^{-2}$ $s^{-1}$) see eqn. (3) |
| $E$ | activation energy |
| $R$ | gas constant |
| $\Delta H$ | the heat of reaction (J $mol^{-1}$) |
| $H$ | the heat of reaciton related to unit volume (J $m^{-3}$) |
| $n$ | formal order of reaction |
| $N$ | number of moles |
| $M$ | molar mass of the starting material |
| $\rho$ | density of the starting material |
| $\dot{Q}_v$, $\dot{Q}_\lambda$ | heat flux, expressed by the rate of the reaction and heat conduction, respectively |
| $\beta$ | heating rate |
| $\lambda$, $\lambda_{min}$ | thermal conductivity and its minimum value providing a selected accuracy of estimated kinetic parameters, see eqn. (21) |
| $l$ | the maximum difference between the temperature of the reacting interface and the program temperature |

*Parameters of the iteration procedure*

| | |
|---|---|
| $T'(r_0)$, $t'$,<br>$v'$, $r'$ | the values of $T(r_0)$, $T$, $v$ and $r$ at time $t - \Delta t$ |
| $T_i$ | the temperature of the reacting phase boundary calculated in the $i$-th iteration cycle |
| $\epsilon$ | a preselected small temperature difference |

*Empirical parameters characterizing the shape of the peak (see also refs. 15–17)*

| | |
|---|---|
| $T$(Max) | program temperature at the maximum $d\alpha/dt$ |
| $T(\alpha)$ | program temperature relevant to $\alpha$ |

| | |
|---|---|
| $\Delta T(\alpha_2, \alpha_1)$ | $T(\alpha_2) - T(\alpha_1)$ |
| $M_{1R}$ | the first relative moment of the peak, i.e. the program temperature belonging to the center of gravity of the peak |
| $W$ | the reciprocal of the maximum rate, $[\mathrm{d}\alpha/\mathrm{d}T(r_0)]_{\mathrm{Max}}^{-1}$ |
| $\alpha(\mathrm{Max})$ | the reacted fraction at the peak maximum |
| $R(0.6)$ | $\Delta T(0.6, 0.2)/\Delta T(0.8, 0.2)$ |
| $U$ | $\Delta T(0.8, 0.2)/W$ |

*Symbols used in dimension analysis*

$[L]$ length
$[\theta]$ time
$[T]$ temperature
$[E]$ energy
$a$, $b$, $c$,
$d$, $e$ exponents in eqn. (15)
$a'$, $b'$,
$c'$, $d'$ exponents in eqn. (21)

## REFERENCES

1 J. Šesták, Thermophysical properties of solids. Their measurements and theoretical thermal analysis, in G. Svehla (Ed.), Wilson and Wilson's Comprehensive Analytical Chemistry, Vol. XII(D), Elsevier, Amsterdam, 1984.
2 Gy. Pokol, S. Gál, J. Sztatisz, L. Domokos and E. Pungor, in J. Wood et al. (Eds.), Reactivity of Solids, Proc. 8th Int. Conf., Göteborg, Plenum Press, New York, 1977, p. 209.
3 Gy. Pokol, S. Gál and E. Pungor, Thermochim. Acta, 33 (1979) 259.
4 Gy. Pokol, J. Therm. Anal., 23 (1982) 235.
5 J. Šesták and G. Berggren, Thermochim. Acta, 3 (1971) 1.
6 F. Paulik and J. Paulik, J. Therm. Anal., 5 (1973) 253.
7 A.L. Draper and L.K. Sveum, Thermochim. Acta, 1 (1970) 345.
8 K. Seybold, T. Meisel and T. Cserfalvi, J. Therm. Anal., 15 (1979) 93.
9 K. Seybold, T. Meisel and T. Cserfalvi, in H. Chihara (Ed.), Thermal Analysis, Proc. 5th Int. Conf., Kyoto, Kagaku Gijutsu-Sha, Tokyo, 1977, p. 416.
10 J. Şesták, Talanta, 13 (1966) 567.
11 G. Várhegyi, Thermochim. Acta, 59 (1982) 31.
12 G. Várhegyi, Thermochim. Acta, 59 (1982) 43.
13 G. Várhegyi, Thermochim. Acta, 65 (1983) 333.
14 L. Reich and S.S. Stivala, Thermochim. Acta, 1 (1970) 65.
15 Gy. Pokol and S. Gál, Anal. Chim. Acta, 167 (1985) 183.
16 Gy. Pokol, S. Gál and E. Pungor, Anal. Chim. Acta, 167 (1985) 193.
17 Gy. Pokol, S. Gál and E. Pungor, Anal. Chim. Acta, 175 (1985) 289.
18 Gy. Pokol, S. Gál and E. Pungor, in Proc. 8th Int. Conf. Thermal Analysis, Thermochim. Acta, 92 (1985) 89.
19 R.H. Perry, C.H. Chilton and S.D. Kirkpatrick (Eds.), Chemical Engineers' Handbook, 4th edn., McGraw-Hill, New York, 1965.